

Mat. Res. Soc. Symp. Proc. Vol. 718 (Perovskite Materials) 25-33 (2002)

## Structural Aspects of Magnetic Coupling in $\text{CaCu}_3\text{Mn}_4\text{O}_{12}$ and $\text{CaCu}_3\text{Ti}_4\text{O}_{12}$

M. D. Johannes,<sup>1</sup> W. E. Pickett<sup>1</sup>, and R. Weht<sup>2</sup>

<sup>1</sup>*Department of Physics, University of California, Davis CA 95616 and*

<sup>2</sup>*Departamento de Física, CNEA,  
Avda. General Paz y Constituyentes,  
1650 - San Martín, Argentina*

### Abstract

Two perovskite-derived materials,  $\text{CaCu}_3\text{Mn}_4\text{O}_{12}$  and  $\text{CaCu}_3\text{Ti}_4\text{O}_{12}$ , have drawn much recent interest due to their magnetoresistive, dielectric, and magnetoelectronic characteristics. Here we present initial theoretical insights into each of these points, based on first principles, density functional based calculations. Our results predict CCMO to have a spin-asymmetric energy gap, which leads to distinct temperature- and magnetic field-dependent changes in properties, and helps to account for its observed negative magnetoresistivity. We have studied CCTO primarily to gain insight into the exchange coupling in both these compounds, where the conventional superexchange coupling vanishes by symmetry for both nearest and next nearest Cu-Cu neighbors, a consequence of the structure. In CCTO, it is necessary to go to 5th Cu-Cu neighbors to obtain a (superexchange) coupling that can provide the coupling necessary to give three dimensional order. Non-superexchange mechanisms may be necessary to describe the magnetic coupling in this structural class.

### INTRODUCTION

The mineral  $\text{CaTiO}_3$ , discovered in 1839 in the Ural Mountains and named after Count von Perovski, is the prototype of what has since been found to be a large class of  $\text{ABO}_3$  perovskite materials. The ideal structure has a simple cubic Bravais lattice with A atoms on the corners, B atoms at the center, and oxygens on the face. Alternatively, the structure is made up of  $\text{BO}_6$  corner-shared octahedra, with the A atom placed in the interstitial regions between eight octahedra. This latter picture of corner-shared octahedra has strong theoretical backing and great structural utility, because many of the structural variations observed in perovskites can be characterized simply as collective rotations (or at high temperature, incoherent ones) of the octahedra.

Here we will address a class with a quadrupled perovskite structure, in which four  $\text{ABO}_3$  units comprise the primitive cell.[1] This structural class [2] can be obtained from the ideal structure (1) by replacing three out of every four A site ions (nearly always closed shell ions) with an  $A'$  ion, which quadruples the cell to  $AA'_3B_4O_{12}$ , and then (2) performing a correlated rotation of the four octahedra, each around one of the  $\langle 111 \rangle$  axes, until the  $A'$  ion is fourfold coordinated with O ions in a nearly square arrangement. This tilt-

ing leaves one triangular face of each octahedra perpendicular to a (111) axis of the cubic lattice (Fig. 1). The need for a Jahn-Teller ion as the  $A'$  ion was recognized early on; especially for  $A' = \text{Cu}^{2+}$ , this distortion leaves it with the square planar configuration it commonly demands. The  $\text{Mn}^{2+}$  ion is also found in the  $A'$  position in this structure.

In this paper we will address the electronic and magnetic structure of two of these compounds, the hybrid cupromanganite  $\text{CaCu}_3\text{Mn}_4\text{O}_{12}$  (CCMO) and the hybrid cuprotitanate  $\text{CaCu}_3\text{Ti}_4\text{O}_{12}$  (CCTO). They are isostructural, with the  $\text{CuO}_4$  plaquettes very nearly square – the bonds connecting Cu and O are all the same length, though the angles between bonds deviate slightly from 90 degrees. Similarly, the distances between the B-site ion (Mn or Ti) and each of its six neighbors are identical, but the angles differ slightly from 90°. Each oxygen now belongs to a single planar  $\text{CuO}_4$  plaquette and to two tilted ( $\text{MnO}_6$  or  $\text{TiO}_6$ ) octahedra.

The additional chemical as well as structural complexity of this quadrupled structure results in behavior that is different than in  $\text{ABO}_3$  perovskites, and some of this behavior may be unique due to the specific stereochemical relationships in this class of materials. The  $\text{Cu}^{2+}$

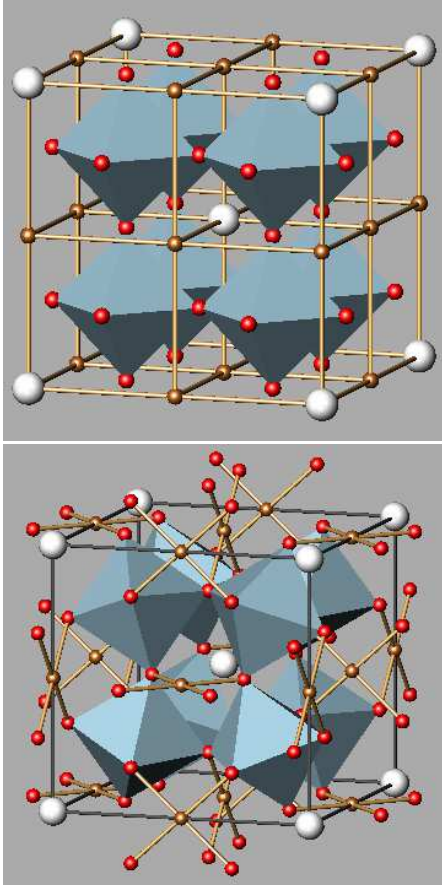


FIG. 1: **The quadrupled perovskite structure.** *Top* The original perovskite structure is still obvious, despite the replacement of  $\frac{3}{4}$  of the A-site ions. *Bottom* Tilted octahedra allow oxygens to form  $\text{CuO}_4$  plaquettes with copper ions.

ion in this structure has been discussed in a Jahn-Teller context by Lacroix[4], however, it is so far removed in this structure from quasi-cubic symmetry that this viewpoint is limited in utility. The necessity of a Jahn-Teller ion in this site strongly promotes stoichiometry, certainly in the Cu site but apparently overall – no significant deviation from stoichiometry could be detected in  $\text{CaCu}_3\text{Ti}_4\text{O}_{12}$  and  $\text{CdCu}_3\text{Ti}_4\text{O}_{12}$ , where thorough structural studies have been possible.[5, 6, 7]

$\text{CaCu}_3\text{Mn}_4\text{O}_{12}$  (CCMO), a magnetic semiconductor, combines the functional unit of the high temperature superconductors – the square  $\text{CuO}_4$  plaquette – with the functional unit of the colossal magnetoresistance (CMR) manganites – the  $\text{MnO}_6$  octahedron – in a coherent (periodic)

manner. So far it is available only in polycrystalline form, where it displays a substantial negative magnetoresistance (MR) beginning from its magnetic ordering temperature of 370 K down to low temperature, where its MR reaches -40%. [8] Formally, two magnetic ions  $\text{Mn}^{4+}$  ( $d^3, S = \frac{3}{2}$ ) and  $\text{Cu}^{2+}$  ( $d^9, S = \frac{1}{2}$ ) are anticipated, and magnetic ordering is observed at 355 K. The Cu and Mn magnetic moments are antialigned, resulting in a ferrimagnetic configuration. The (polycrystalline) resistivity  $\rho(T)$  is semiconducting in magnitude and also in temperature derivative, but showed no visible anomaly upon ordering, [8] so unlike in many manganites there is no insulator-metal transition accompanying magnetic ordering. The magnetization  $M(T)$  shows a steep, apparently first-order jump at  $T_C$  to  $\sim 80\%$  of its saturation value. The temperature dependence of the activated resistivity (over a limited temperature range) was fitted to obtain an energy gap (actually, an activation energy) of  $\sim 0.12$  eV.

CCTO has gathered recent interest due to its unusual dielectric properties. At frequencies around 1 kHz, the extremely high dielectric constant ( $\epsilon \approx 10^4$ ) is nearly temperature independent between 25 and 300 C.[5, 9, 10] It is an antiferromagnetic (AFM) insulator with an experimental gap of 1.5 eV as a lower limit. (see ref. 20 in [11]) The AFM ordering is three-dimensional and has a Néel temperature of 25K.[12, 13, 14] The magnetic order of the  $\text{Cu}^{2+}$  ions is Néel-like with each being antialigned with its nearest neighbor on the (one-quarter depleted by Ca) simple cubic lattice. The Ti ions can have no net polarization by symmetry. The formal valency of these ions is  $d^0$ , but our calculations show that some amount of Ti 3d charge is present and is involved in magnetic coupling.

## CALCULATIONAL METHODS

Calculations were carried out using the full-potential linearized augmented plane wave (FLAPW) method in the WIEN97 [15] implementation. The exchange-correlation potential of Perdew and Wang (92) [16] was used and over 2000 LAPW's were employed in the basis set. In transition metal oxides, there is often the ques-

tion of whether corrections to the local density approximation are necessary to obtain a reasonable description, with the answer being guided by experimental data. While we suspect some corrections will be necessary for both of these compounds, the results we have obtained have the right magnetic character and are insulating, hence we expect they are useful in beginning the interpretation of their observed behavior. The experimental lattice parameter and ionic positions were used: for CCMO,  $a = 7.241 \text{ \AA}$ , ( $y = 0.3033, z = 0.1822$ ) for the O position; for CCTO,  $a = 7.3843 \text{ \AA}$ , ( $y = 0.3033, z = 0.1790$ ) for the O position. The crystallographic space group is  $\text{Im}\bar{3}$  but in order to reproduce the experimentally observed AFM order for CCTO, the unit cell had to be doubled. This results in a simple cubic cell; space group  $\text{Pm}\bar{3}$ . The calculation was performed first using the fixed-spin moment procedure [17], with the moment held to zero. Once a reasonable charge density was reached, the calculation was allowed to proceed to self-consistency with no restriction on overall moment. The final moment indeed converged to zero and an anti-ferromagnetic ground state resulted. For CCMO, the calculation was begun with aligned Mn and Cu moments. However, the Cu moment flipped during iteration, and only a ferrimagnetic magnetic arrangement was obtained.

## CCMO

### Electronic structure

The calculated majority and minority band structures in the vicinity of the gap are shown in Fig. 2. The calculated energy gaps are 0.50 eV for spin up (parallel to the net magnetization) and of 0.18 eV for spin down, both direct. For the minority carriers the gap occurs at H between pure Cu  $d_{xy}$  states below the gap to Mn  $t_{2g}$  character above. The small thermal gap, 0.09 eV, is *indirect* between the spin down valence band maximum at H and the spin up conduction band minimum at  $\Gamma$ . It is common for the band gap in density functional calculations to be smaller than the true gap, but the band character and shape on either side of the gap typically are given reasonably. In this case the calculated

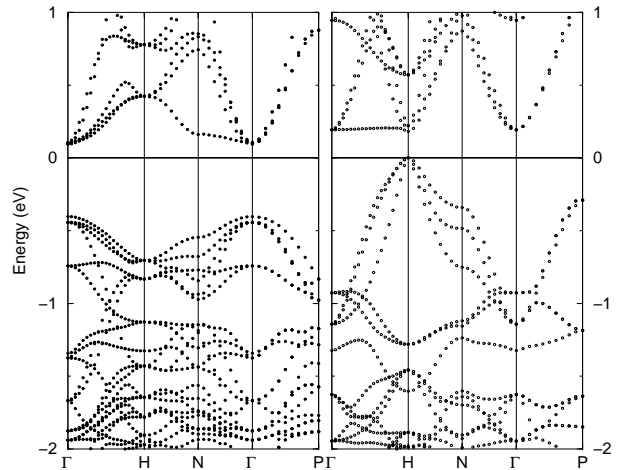


FIG. 2: **Bandstructure of CCMO in the region of the fundamental gap.** The indirect thermal gap is between the spin-down states at the H point (right panel) to the spin-up states at  $\Gamma$  (left panel)

gap is quite similar to the quoted experimental value.

As in many related cuprates, the hole in the Cu  $3d$  shell (the magnetic orbital) involves the  $dp\sigma$  antibonding combination of the Cu  $d_{xy}$  and the four neighboring O  $p\sigma$  orbitals, a Wannier function which we denote as  $\mathcal{D}_{xy}$ . The other Cu  $d$  orbitals are concentrated in a small region between 1 and 2.5 eV below the gap. If the  $\text{CuO}_4$  unit were actually a square,  $\mathcal{D}_{xy}$  would not couple with other Cu  $d - \text{O } p$  combinations, and this is a good approximation. From the structural figures, it is clear that  $\mathcal{D}_{xy}$  functions on both near neighbor and second neighbor Cu are orthogonal by symmetry. As a result, the dispersion involves further neighbors as well as Mn-centered Wannier functions, and becomes difficult to model with a tight-binding approach, (see the sections on CCTO, below).

### Magnetic ordering and character

The calculated moments inside the muffin tin spheres are  $2.42 \mu_B$  and  $-0.45 \mu_B$  for Mn and Cu respectively. The idealized values ( $S = \frac{3}{2}$ ,  $3 \mu_B$  for Mn and  $S = \frac{1}{2}$ ,  $1 \mu_B$  for Cu) are reduced due to hybridization with the O  $2p$  states, as observed in other transition metal oxides. The

net magnetic moment of  $9 \mu_B$  per formula unit is however what would be obtained from the formal moments aligned ferrimagnetically. The magnetic moment on the Cu ion is a result of the exchange splitting and resulting single occupation of the  $\mathcal{D}_{xy}$  orbital. Magnetism in the Mn ion comes as expected from the splitting of the  $t_{2g}$  orbitals and filling only of the spin up states.

The magnetism of  $\text{CaCu}_3\text{Mn}_4\text{O}_{12}$  presents several interesting questions. First of all, the exchange splitting of the Cu  $\mathcal{D}$  orbital is  $\Delta_{ex}^{Cu} \sim 1.2$  eV. Although such exchange splittings are less apparent in ferrimagnets than in simple ferromagnets, this Cu  $d$  orbital is separate from the other Cu  $d$  orbitals, making it easy to identify the splitting from the density of states. Given its moment of  $m_{Cu} = 0.45 \mu_B$  (inside its muffin tin sphere), there results a ratio  $\Delta_{xy}^{Cu}/m_{Cu} = 2.7 \text{ eV}/\mu_B$ , a very large value considering this ratio (the Stoner  $I_{xy}^{Cu}$  in the relation  $\Delta_{ex} = Im$ ) is usually no more than  $1 \text{ eV}/\mu_B$  in transition metal magnets. The exchange splitting of the other Cu  $d$  orbitals is smaller, of the order of 0.4 eV. This difference reflects a strongly anisotropic exchange potential on the Cu ion, which bears further study.

The magnetic coupling in  $\text{CaCu}_3\text{Mn}_4\text{O}_{12}$  is potentially quite complex to unravel due to the presence of two types of magnetic ions and the large cell with low symmetry sites. The various bond angles involved in the exchange processes in  $\text{CaCu}_3\text{Mn}_4\text{O}_{12}$  have been discussed in our earlier paper,[19] and there may be alternative insights to be gained first – these are addressed below in the discussion of CCTO. Furthermore, Mn-Mn coupling is involved as well as the Mn-Cu coupling discussed in the previous section. Since Mn spins lie on a simple cubic lattice connected by a single  $\text{O}^{2-}$  ion, the Goodenough-Kanamori-Anderson (GKA) rules can be applied to understand  $J^{Mn-Mn}$  of ferromagnetic sign. Further Mn-Mn couplings should be small and not affect qualitative behavior. Whereas  $180^\circ \text{ Mn}^{4+}\text{-O-Mn}^{4+}$  coupling is antiferromagnetic (*viz.*  $\text{CaMnO}_3$ ), when this angle is reduced to  $142^\circ$  a ferromagnetic sign may result from the GKA rules. Parallel alignment of the Mn spins is observed, and is the only situation we have encountered in our calculations. Finally, there is the question of

the origin of the AFM Mn-Cu coupling. In this structure all oxygen ions are equivalent and each one is coordinated with two Mn ions and one Cu ion. As discussed elsewhere,[19] if only nearest neighbor Mn-Cu coupling is appreciable, it is AFM in sign and  $\approx 20 \text{ meV}$ . Cu-Cu coupling in this structure is discussed in the next section.

### Transport behavior.

Several unusual aspects of transport and of thermally-induced carriers in CCMO have been discussed previously. The main experimental interest so far has been in the magnetoresistance, becoming appreciable as it does above room temperature and continuing (indeed, increasing) to low temperature.[8] Due to the 100% spin polarization of thermally induced or doped-in carriers in a spin-asymmetric semiconductor such as we predict CCMO to be, intergrain transport is very strongly dependent on the direction of magnetization of neighboring grains. The effect is directly analogous to arguments applied to granular half-metallic ferromagnetic materials. The consequences have been discussed by several authors; see in particular the review by Ziese.[20] A magnetoresistance of 30-40%, as seen in CCMO at low temperature, is readily accounted for by the alignment by the field of grains with fully polarized carriers.

### CCTO

Our calculation correctly reproduces the observed AFM insulating character of CCTO. The gap in the bandstructure, shown in Fig.3 is only 0.2 eV, considerably smaller than the experimental value, but such underestimation of the gap is common in LDA calculations and arises from underestimation of correlation effects. Our density of states is similar to that presented by He et al. [11] The band structure reflects the six bands, associated with six Cu ions, that are responsible for the magnetism of the compound. These states are the same  $\mathcal{D}_{xy}$  Wannier orbitals introduced in the discussion of CCMO above. Since these six bands are separated from other bands, they are

good candidates for providing a minimalist representation of the origin of magnetic coupling. The bands are fit to a tight-binding model and the hopping amplitudes are used to obtain the spin-spin coupling  $J = \frac{4t^2}{U}$  via the superexchange mechanism. This prescription has worked well in several structurally complicated magnetic insulators such as  $\text{CuV}_4\text{O}_9$ , [21]  $\text{Li}_2\text{CuO}_2$ , [22] and  $\text{LiVOSiO}_4$ . [23] Sometimes, however, a multi-orbital model may be required. [24] An analysis of the character of these half-filled bands shows that they contain some Ti  $3d$  character in addition to the expected Cu  $d$ , O  $p$  antibonding character, and therefore that the Ti (nominally  $d^0$  ion) is involved in the magnetic coupling.

### Tight-Binding Model.

The most basic tight-binding model includes only the  $D_{xy}$  Wannier functions centered on each of the six Cu sites in the AFM cell. The Wannier functions on different sites are orthogonal, and they have the symmetry of the Cu  $d_{xy}$  orbital, which provides essential selection rules. The contributions of many sites are present due to hybridization, and for CCTO contains Ti  $3d$  character, as mentioned above. The hopping parameters may be fit from the bandstructure, in fact, for CCTO it has been possible to use the paramagnetic band structure.

Typically only 1st and 2nd nearest neighbor hopping parameters are required to describe the band dispersion. However, for CCTO the 1st and 2nd Cu-Cu hopping amplitudes (hence superexchange coupling, see below) vanish by symmetry[25]. The 3rd neighbor interactions are non-zero and reproduce the general band dispersion, but important degeneracies are not broken. This can be understood by noticing that CCTO is made up of three separate BCC sublattices, each containing co-planar  $\text{CuO}_4$  squares with their associated Wannier functions. The 3rd neighbor interactions couple only Cu sites within a given sublattice, hence the bands are degenerate at this level of description. Hopping between Cu sites belonging to two non-co-planar  $\text{CuO}_4$  squares is necessary to split the bands. The 4th nearest neighbor interaction is non-zero but, remarkably, again couples only Cu

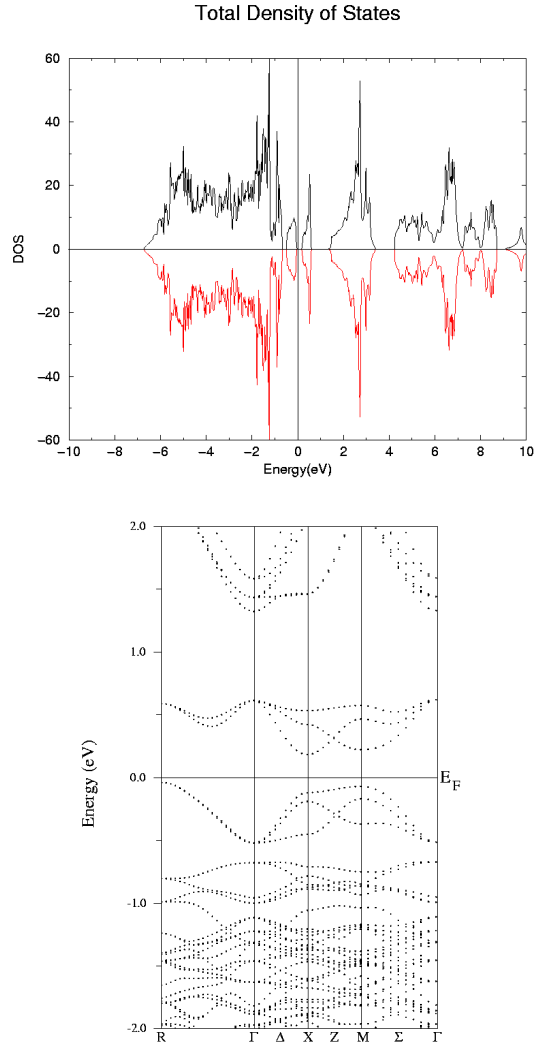


FIG. 3: **CCTO Density of States and Bandstructure.** *Top* The small gap indicates an insulating ground state and the identical spin-up and spin-down densities are consistent with AFM ordering. *Bottom* The six magnetic bands are separated from all others. Three are filled and three are unfilled.

sites within a single sublattice. Only at 5th neighbor is there non-zero hopping between different sublattices. This hopping involves Cu sites which are separated by more than a lattice constant (which itself is twice a conventional perovskite lattice constant!) but it is essential in order to obtain hopping (and therefore superexchange coupling) between the three sublattices. To reproduce the band structure accurately, it is necessary to include 7th neighbors. Although this 7th neighbor interaction again couples Cu

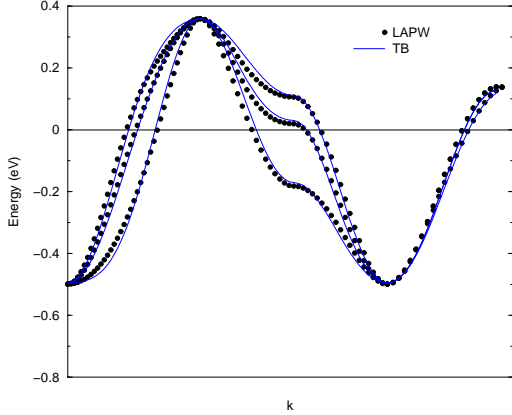


FIG. 4: **LAPW vs. Tight-Binding Bandstructure.** The tight-binding fit includes up to 7th neighbor parameters. This produces a bandstructure remarkably similar to the all-electron LAPW calculation.

sites only within each sublattice, it clearly contributes non-negligibly to the observed dispersion. Including all non-zero interactions up to 7th neighbor yields a very accurate bandstructure. (Fig.4) The hopping parameters used to make this fit are as follows:

$t_{3rd}$	-53.0 meV
$t_{4th}$ $\pi$ (Ca)	-51.0 meV
$t_{4th'}$ $\pi$ (no Ca)	16.3 meV
$t_{4th''}$ $\delta$	20.1 meV
$t_{5th}$	5.6 meV
$t_{6th}$	-.7 meV
$t_{7th}$ $\sigma$	-1.4 meV
$t_{7th'}$ $\delta$ (Ca)	2.7 meV
$t_{7th''}$ $\delta$ (no Ca)	-9.5 meV

For both 4th and 7th neighbors, there are several different parameters. This is for one of two reasons. In some cases, the Wannier orbitals involved in these hopping terms are oriented differently with respect to one another along different directions (i.e. towards different neighbors of the same distance) which produces a different magnitude of hopping. In other cases, the chemical environment is actually different, such that the path from one orbital to another along one direction requires going through

a Ca while along a second direction it does not. The orientation differences are indicated using the common chemical bonding labels and the chemical differences are noted by stating whether or not Ca ions are involved. The little information for exchange coupling in CCTO to date is from magnetic Raman spectroscopy. Koitzsch et al. [13] fit magnetic excitations to 1st, 2nd, and 3rd neighbor exchange couplings, which allows no reasonable comparison with our values. Linear spin wave calculations are in progress that will allow closer comparison with experiment.

### Magnetic Order

Since the Cu ion has spin half, there is no first order single ion anisotropy and the spin behavior should be Heisenberg-like. Using the tight-binding hopping parameters, the Heisenberg model based on superexchange coupling may be formulated, the notation being standard:

$$H = \sum_{\langle i,j \rangle} J_{ij} \vec{S}_i \cdot \vec{S}_j \quad J_{ij} = \frac{4t_{ij}^2}{U} \quad (1)$$

The on-site repulsion  $U$  is taken to be 4.0 eV, as similar values have been used for such “single band” representations of cuprates. The magnetic order that results from applying this model has no dependency on the value of  $U$ , except that it be large enough to justify the use of the Heisenberg model ( $t^2 \ll U$ ). The value of  $U$  (i.e.  $J$ ) will however affect the ordering temperature. Regardless of the sign of  $t_{ij}$ ,  $J_{ij}$  from this superexchange treatment will be positive (favoring opposite alignment of the two spins).

Using this observation, it is clear that  $J_{3rd}$  will anti-align a given spin with its third nearest neighbor, as is observed. However, as noted above, this coupling is only between spins on the same sublattice so although it results in sublattice ordering, there is no alignment of sublattices with respect to one another. The next coupling,  $J_{4th}$  wants to anti-align the spin with its 4th nearest neighbor. However, 4th nearest neighbors share a third neighbor with which they are already anti-aligned. The system is therefore frustrated. The largest  $J_{4th}$  is slightly smaller

than  $J_{3rd}$  and there are only two such neighbors as compared to the eight of  $J_{3rd}$ . Thus at this level, all sublattices are antialigned internally, though with some frustration. Intersublattice coupling occurs because  $J_{5th}$  antialigns a given spin with its 5th neighbor, in effect antialigning nearest neighbors, thereby correctly reproducing the three-dimensional anti-ferromagnetic order of CCTO. In this picture, then, full three-dimensional AFM order depends on interactions as far away as 5th Cu neighbors, which are actually separated by many more than five ions.

## CONCLUSIONS

Ferrimagnetic order has been calculated for CCMO with total moment of  $9\mu_B$  per formula unit, consistent with experiment. The predicted spin-asymmetric gap leads to 100% spin polarized carriers that may be essential in accounting for its large and weakly temperature dependent magnetoresistance. The superexchange picture of magnetism has been applied to CCTO, and suggests that extremely long-range interactions are important and perhaps even responsible for the AFM order. Within this model, there is an energy advantage (for classical spins) of  $\sim 23$  meV/Cu favoring AFM over FM alignment. Though mechanisms besides superexchange may be important to fully understand the magnetism of this compound, this simple picture is able to account for the experimentally observed order.

## ACKNOWLEDGMENTS

We are grateful to C.C. Homes, A.P. Ramirez, S.M. Shapiro, and M. Subramanian for discussions and communication of unpublished work. We benefitted greatly from input on the tight-binding procedure for CCTO from Wei Ku. This work was supported by NSF grant DMR-0114818.

see for example N. Mansourian-Hadavi *et al.*, J. Solid State Chem. **155**, 216 (2000). Our description and figures will make clear the class we are discussing.

- [2] J. Chenavas, J. C. Joubert, M. Marezio, and B. Bochu, J. Solid State Chem. **14**, 25 (1975); J. C. Joubert *et al.*, *Ferrites*, Proceedings of the Third Intl. Conf. on Ferrites, Kyoto 1980 (Reidel, Dordrecht, Netherlands, 1982), p.400.
- [3] A. Collomb *et al.*, J. Magn. Magn. Mat. **7**, 1 (1978).
- [4] C. Lacroix, J. Phys. C **13**, 5125 (1980).
- [5] M.A. Subramanian *et al.*, J. Solid State Chem. **151**, 323 (2000); A.P. Ramirez *et al.* Solid State Commun. **115** 217 (2000)
- [6] C.C. Homes (unpublished work)
- [7] M.A. Subramanian (unpublished work)
- [8] Z. Zeng *et al.*, J. Solid State Chem. **147**, 185 (1999).
- [9] D.C. Sinclair *et al.*, Appl. Phys. Lett. **80**, 2153 (2002).
- [10] C.C. Homes *et al.*, Science **293**, 673 (2001).
- [11] L. He *et al.*, cond-mat /0110166
- [12] A. Collomb, D. Samaras, B. Bochu and J. C. Joubert, Phys. Stat. Solidi (a) **41**, 459 (1977).
- [13] A. Koitsch *et al.*, Phys. Rev. B **65**, 052406 (2002).
- [14] Y.J. Kim *et al.*, Solid State Commun. **121**, 625 (2002)
- [15] WIEN97, see P. Blaha, K. Schwarz, and J. Luitz, Vienna University of Technology, 1997, improved and updated version of the original copyrighted WIEN code, which was published by P. Blaha, K. Schwarz, P. Sorantin, and S. B. Trickey, Comput. Phys. Commun. **59**, 399 (1990);
- [16] J.P. Perdew, Y. Wang PRB, **45**, 13244 (1992).
- [17] K. Schwarz and P. Mohn, J. Phys. F **14**, L129 (1984).
- [18] B. Bochu *et al.*, J. Magn. Magn. Mat. **15-18**, 1319 (1980).
- [19] R. Weht and W. E. Pickett, Phys. Rev. B **65**, 014415 (2001).
- [20] M. Ziese, Rep. Prog. Phys. **65**, 143 (2002).
- [21] C.S. Hellberg *et al.*, J. Phys. Soc. Japan **68**, 3489 (1999)
- [22] R. Weht and W.E. Pickett, Phys. Rev. Lett. **80**, 2502 (1988)
- [23] H. Rosner *et al.*, Phys. Rev. Lett. **88**, 186405 (2002).
- [24] S. Feldkemper *et al.*, Phys. Rev. B **52**, 313 (1995)
- [25] J.C. Slater, G.F. Koster, Phys. Rev. **94** 844 (1954).

---

[1] The term “quadrupled perovskite structure” has also been used for a different (layered and oxygen deficient) class of oxide defect compounds;